Biochemical and Biophysical Research Communications 601 (2022) 38–44

Contents lists available at ScienceDirect

Biochemical and Biophysical Research Communications

journal homepage: www.elsevier.com/locate/ybbrc

Efferocytosis and enhanced FPR2 expression following apoptotic cell instillation attenuate radiation-induced lung inflammation and fibrosis

Sang Yeon Kim [a], Jin-Mo Kim [a, b], Son Ro Lee [a], Hyun-Jin Kim [a], Jae Hee Lee [a], Ho Lim Choi [a], Yoon-Jin Lee [c], Yun-Sil Lee [d], Jaeho Cho [a, *]

[a] Department of Radiation Oncology, Yonsei University College of Medicine, 50-1 Yonsei-ro, Seodaemun-gu, Seoul, 03722, South Korea
[b] Department of Manufacturing Pharmacy, Natural Product Research Institute, College of Pharmacy, Seoul National University, Seoul, South Korea
[c] Korea Institute of Radiological and Medical Science, Seoul, South Korea
[d] Graduate School of Pharmaceutical Science, Ewha Womans University, Seoul, South Korea

ARTICLE INFO

Article history:
Received 28 December 2021
Received in revised form
15 February 2022
Accepted 19 February 2022
Available online 21 February 2022

Keywords:
Formyl peptide receptor 2
Efferocytosis
Irradiation
Lung inflammation
Lung fibrosis

ABSTRACT

Lung inflammation and fibrosis are common side effects of radiotherapy that can lead to serious reduction in the quality of life of patients. However, no effective treatment is available, and the mechanisms underlying its pathophysiology are poorly understood. Irradiation increases formyl peptide receptor 2 (FPR2) expression in lung tissue, and FPR2 agonists are known to promote the uptake of apoptosis cells, referred to as efferocytosis that is a hallmark of the resolution of inflammation. Herein, in a mouse model of radiation-induced lung injury (RILI), efferocytosis was induced by injecting apoptotic cells into the lung through the trachea, and its correlation with FPR expression and the effect of efferocytosis and FPR expression on RILI were assessed. Interestingly, when apoptotic cells were injected into the lung, the radiation-induced increase in FPR2 expression was further amplified. In the mouse model of RILI, apoptotic cell instillation reduced the volume of the damaged lung and prevented the decrease in lung function. Additionally, the expression of inflammatory cytokines, fibrosis-related markers, and oxidative stress-related markers was reduced by apoptotic cell instillation. Co-administration of apoptotic Jurkat cells and WRW4, the FPR2 antagonist, reversed these effects. These findings suggest that efferocytosis induced by apoptotic cell instillation and enhanced FPR2 expression attenuate RILI, thereby alleviating lung inflammation and fibrosis.

1. Introduction

Pulmonary fibrosis has been widely examined in recent years as our understanding of it has changed from characterising it as a chronic non-specific disease to a specific disease that is frequently caused by various environmental factors. Genetic variation induced by factors such as reactive oxygen species (ROS), bacteria, viruses, and radiation can cause deformation of immune, vascular, and epithelial cells in a process that involves numerous cytokines and growth factors during chronic inflammation [1]. Recently, anti-inflammatory therapy has been shown to attenuate pulmonary fibrosis.

Formyl peptide receptor-2 (FPR2, ALX/FPR2) is a G protein-coupled receptor that transduces signals from lipoxin A4 (LXA4), annexin A1, and serum amyloid A (SAA) to modulate inflammation [2]. ALX/FPR2 overexpression inhibits TGF-β1–induced epithelial-mesenchymal transition (EMT) of lung cancer cells [3], and LXA4 inhibits collagen production, decreases the expression of fibrosis-related proteins and inflammatory cytokines in RILI mouse model [4]. We previously reported that irradiation (IR) regulates LXA4-FPR2 signalling in IR-exposed mouse lung tissue, and WRWWWW (WRW4, antagonist of FPR2) blocked the effect of endogenous LXA4 and enhanced IR-induced NK-κB promoter activity [4].

Efferocytosis or engulfment of apoptotic cells by macrophages is an essential process with roles in tissue homeostasis, embryologic development immunity, and inflammation resolution [5].

Abbreviations: EMT, epithelial-mesenchymal transition; FPR2, formyl peptide receptor-2; IR, irradiation; LXA4, lipoxin A4; RILF, radiation-induced lung fibrosis; RILI, radiation-induced lung injury.

* Corresponding author.
E-mail address: jjhmd@yuhs.ac (J. Cho).

https://doi.org/10.1016/j.bbrc.2022.02.075

Efferocytosis by SAA was mediated specifically by FPR2, one of the SAA receptors [6]. Moreover, efferocytosis increases the levels of anti-inflammatory proteins, such as TGF-β, interleukin (IL)-10, and PPAR-γ and the production of vascular endothelial growth factor and hepatocyte growth factor (HGF), thereby regulating the survival of epithelial and endothelial cells to improve homeostasis [7]. This phenomenon involved in efferocytosis inhibits ROS production and Rho/ROCK activity [8]. Signalling pathways identified as major mechanisms of pulmonary fibrosis include the c-Abl/PKC/FLI-1, AP-1, JAK2/STAST3, and PPAR pathways and involve cytokines, chemokines, and angiogenic, growth, and various other factors [9,10]. Hedgehog inhibitors and SRC family tyrosine kinase inhibitors, used to block the Wnt pathway, were reported as being effective for inhibiting fibrosis by preventing EMT [11]. Additionally, the increased levels of active oxygen due to the action of NADPH oxidases (NOXs) in inflammatory reactions stimulate immune, vascular, and epithelial cells to promote fibrosis [12].

Previously, we developed a mouse model that simulates clinical stereotactic body radiotherapy using an image-guided animal IR system to deliver a single 75-Gy dose to the mouse lung [13] and validated the induction of lung fibrosis following high-dose IR [14]. Herein, we hypothesised that efferocytosis and enhanced expression of FPR2, the LXA4 receptor, by apoptotic cell recognition and clearance programming can reduce RILI. In this study, we first investigated pulmonary functions and characterised FPR2 expression following apoptotic cell instillation in the RILI model. Next, we investigated the changes in anti-inflammatory cytokine levels and measured EMT and ROS marker levels. Our study is expected to increase the possibility of the development of potential therapeutic agents for radiation-induced lung fibrosis (RILF) and contribute to improving the quality of life of patients with RILF.

2. Materials and methods

2.1. Animal experiments

Male C57BL mice aged 6 weeks (Orient Bio, Sungnam, South Korea) were used in all experiments. The Animal Care Committee of Yonsei University Medical School (Seoul, Korea, YUHS-IACUC; 2021-0041) approved the experimental protocol. A single dose of 75 Gy IR was delivered to the left lung using a small-animal irradiator (X-RAD 320; Precision X-Ray, North Branford, CT, USA). Three millimetre collimators were used to mimic clinical stereotactic body radiotherapy conditions with a small IR volume in lung tissues. At two weeks after IR treatment, either saline or 10×10^6 apoptotic Jurkat cells were administered intratracheally. The mice were randomly divided into the following five groups ($n = 3–5$ mice per group): (1) control; (2) IR exposed to a single dose of 75 Gy; (3) IR + Jur (4) IR + Jur + WRW4 treated intravenously with WRW4 (1 mg/kg, 2 weeks after IR) for 4 weeks; and (5) IR + Jur + WRW4.

2.2. Induction of apoptosis

Human lymphocyte Jurkat cells were obtained from the American Type Culture Collection (Manassas, VA, USA) and cultured in RPMI 1640. Apoptosis was induced by ultraviolet radiation at 254 nm for 10 min; the cells were then incubated for 2.5 h before use. Apoptosis was confirmed via flow cytometry after staining with propidium iodide and annexin V (Fig. S1).

2.3. Quantitative reverse transcription polymerase chain reaction (qRT-PCR) analysis

RNA was isolated from the lung tissue using TRIzol™ reagent (15596018, Thermo Fisher, Waltham, MA, USA). Complementary DNA (cDNA) was synthesised using 1 μg of total RNA with a High-Capacity RNA-to-cDNA™ Kit (4388950, Thermo Fisher). qRT-PCR was performed using TaqMan™ Fast Advanced Master Mix (4444963, Thermo Fisher). We measured the expression levels of the FPR2 (Mm00484464-s1, Thermo Fisher) and IL-1β (Mm00434228-m1, Thermo Fisher) genes normalised to that of β-actin (Mm02619580-g1, Thermo Fisher). The relative mRNA levels were calculated using an ABI PRISM7500 (Applied Biosystems, Carlsbad, CA, USA) and analysed using the ΔΔCT method.

2.4. Western blot

Tissues were lysed in RIPA containing protease inhibitors and the phosphatase inhibitor cocktail (GenDEPOT, Baker, TX, USA). Proteins (30 μg) were separated via sodium dodecyl-sulphate gel electrophoresis and transferred onto polyvinylidene fluoride membranes (GE Healthcare, Little Chalfont, UK). The primary antibodies used were α-smooth muscle actin (α-SMA), NOX4, IL-1β, TGF-β1(ab7817, ab154244, ab9722, ab92486, Abcam, Cambridge, UK), FPR2 (NLS1878, Novus Biological, Littleton, CO, USA), ROCK1, N-cadherin, vimentin (4035, 13116, 5741, Cell signaling, Danvers, Massachusetts, USA), twist (gtx127310, Gene Tex, CA, USA), NF-κB, and GAPDH (sc-8008, sc-47724, Santa Cruz Biotechnology, Dallas, TX, USA).

2.5. Human tissues analysis

The study of specimens from patients with RILF was approved by Severance Hospital, Yonsei University (Seoul, Korea, YUHS IRB; 4-2014-0193).

2.6. Histological and immunohistochemical (IHC) analysis

For histological analysis, sections were stained with haematoxylin and eosin (HE) and Masson trichrome (MT). IHC staining was performed using FPR2 (NLS1878, Novus), S100A9, IL-1β, 8-hydroxy-2′-deoxyguanosine (8-OHdG) (ab22506, ab9722, ab48508, Abcam) and α-SMA (M0851, Dako, Glostrup, Denmark). Images were quantified using ImageJ software (ver.2).

2.7. Micro-computed tomographic (CT) analysis

Micro-CT images were acquired using a volumetric CT scanner (NFRPolaris-G90MVC: NanoFocusRay, Iksan, South Korea) at 50 kVp, 180 μA, and 150 mGy (number of views, 700; frame rate, 142 ms). Images were reconstructed by volumetric cone-beam reconstruction (Feldkamp-Davis–Kress method) in on-line/off-line modes. Volumetric analysis was performed using ImageJ software.

2.8. Functional assessment of the lung

Lung function in IR mice was evaluated using the FlexiVent® system (FlexiVent®; SCIREQ, Montreal, QC, Canada), which measures flow-volume relationships in the respiratory system, according to the manufacturer's instructions. All perturbations were performed sequentially until three acceptable measurements (coefficient of determination >0.95) were recorded for each subject, and the average value was calculated.

2.9. HGF quantification

Bronchoalveolar lavage fluid (BALF) samples were collected with 1 mL syringes containing 1 mL PBS inserted into the exposed

trachea of mice. HGF levels were measured using an HGF ELISA kit (R&D system; Minneapolis, MN, USA) according to the manufacturer's protocol.

2.10. Statistical analyses

Statistical analysis was performed using SPSS ver.25 software (SPSS, Inc., Chicago, IL, USA). Differences between the means of multiple groups were evaluated via one-way analysis of variance. The threshold for significance was $p < 0.05$, and all values were expressed as the mean ± standard deviation.

3. Results

3.1. Efferocytic ability of macrophages and anti-inflammatory changes in RILI

To confirm whether efferocytosis was induced and to measure efferocytic ability, we investigated CD68 as a typical phagocytosis marker and S100A9 as a macrophage marker. After IR, inflammatory cells infiltrated the IR foci. In the IR + Jur group, inflammatory cell numbers were significantly reduced ($p < 0.001$) compared to those in the IR, IR + Jur + WRW4, and IR + WRW4 groups (Fig. 1A and B). Phagocytosis increased in the IR + Jur group (Fig. 1A). When WRW4 was co-administered with apoptotic Jurkat cells to inhibit FPR2 activity and induce efferocytosis (IR + Jur + WRW4 group), phagocytosis was significantly reduced and macrophage numbers increased (Fig. 1A and B). When efferocytosis is induced, the expression of HGF increases [15]. In the IR + Jur group, HGF levels in IR-lung tissues significantly increased ($p < 0.05$) compared to that in the IR group. However, in the IR, IR + Jur + WRW4, and IR + WRW4 groups, there were no changes in HGF levels (Fig. 1C). These data showed that the increase in HGF levels is affected by efferocytosis.

3.2. Enhancement of FPR2 expression following apoptotic cell instillation into mice with RILI

We hypothesised that there might be a connection between efferocytosis and FPR2 expression, and we investigated the lung tissue, protein and mRNA levels of FPR2 to determine whether efferocytosis affected FPR2 expression and also examined the tissue of lung cancer patients. Immunohistochemistry results revealed that FPR2 expression in the IR + Jur group was significantly increased compared with that in the IR group ($p < 0.001$, Fig. 2A and B), and the mRNA level of FPR2 in the IR + Jur group was significantly higher than that in the IR group ($p < 0.05$, Fig. 2. C). Western blotting also revealed increased FPR2 expression in the IR + Jur group (Fig. 2D). Interestingly, in the WRW4-treated group, FPR2 expression was significantly reduced compared with that in the IR + Jur group ($p < 0.05$, Fig. 2A and B).

Next, we examined FPR2 expression by assuming a clinical relationship between fibrosis and FPR2 expression in tissue from patients with RILF. Fibrotic tissues of lung cancer patients who underwent surgery following radiotherapy for lung adenocarcinoma were selected based on MT staining. In MT staining, collagen was deposited due to fibrosis and stained blue, and FPR2 expression was also confirmed at the site where fibrosis occurred (Fig. 2E).

3.3. Apoptotic Jurkat cell instillation attenuated RILF and rescued lung function

Six weeks after IR, lung consolidation was observed in all IR groups, whereas only apoptotic Jurkat cell–instilled mice showed

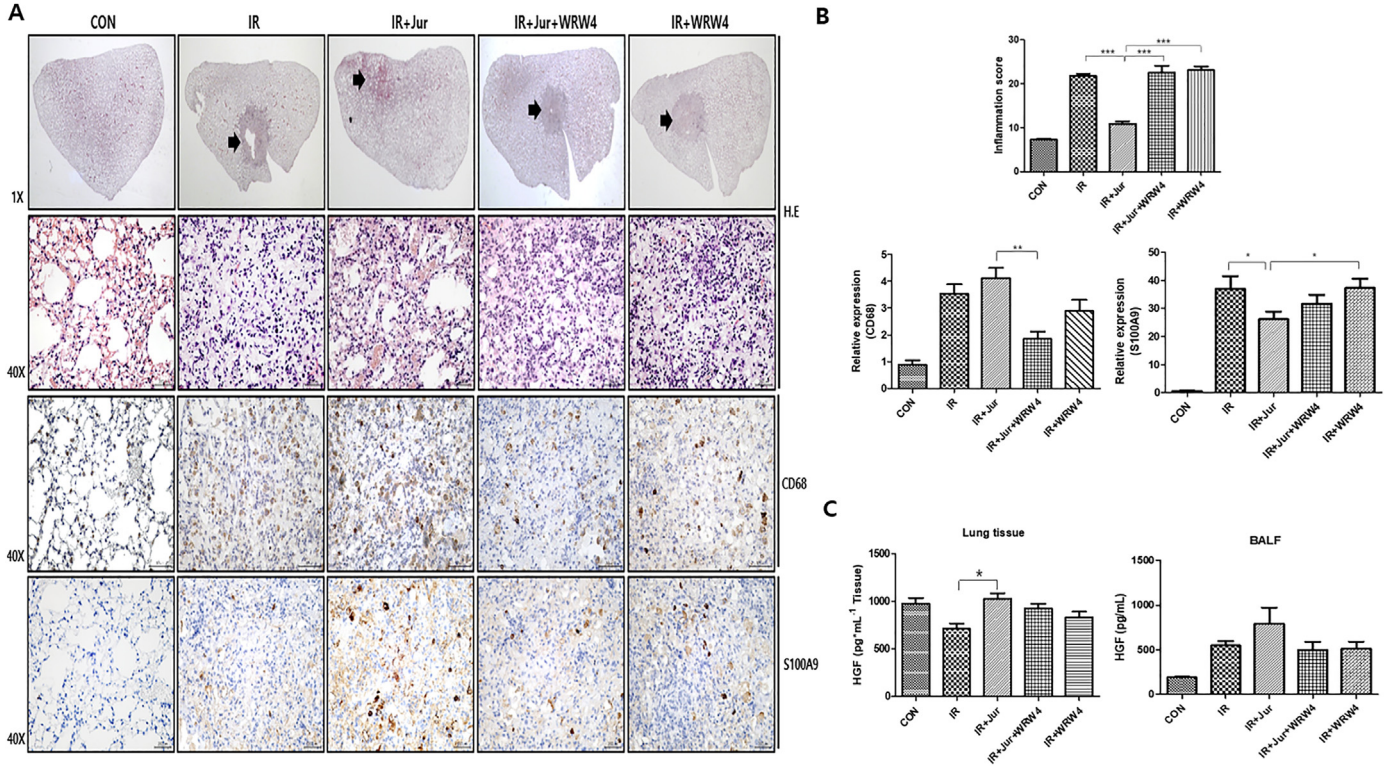

Fig. 1. Changes in phagocytosis and macrophage expression following apoptotic Jurkat cell instillation. (A) Representative HE and Immunohistostaining image of irradiated lung tissues stained with antibodies against CD68 and S100A9. Magnification, 1 × and 40 × . (B) Quantification of relative HE-, CD68⁻. and S100A9-stained area. (C) Quantification of HGF from lung tissue and BALF via ELISA. Data are expressed as the mean ± standard deviation (n = 3–5, *$p < 0.05$, **$p < 0.01$, ***$p < 0.001$).

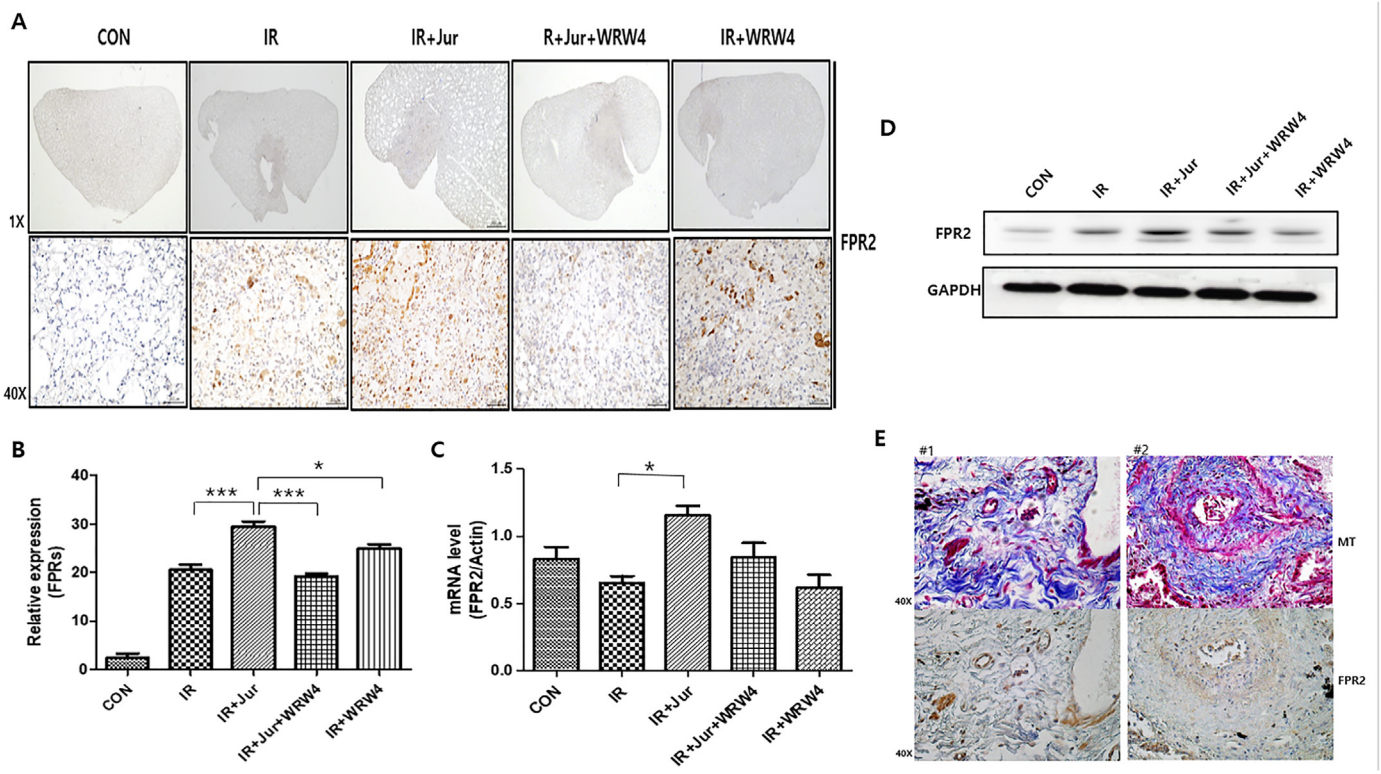

Fig. 2. Instillation of apoptotic Jurkat cells enhances FPR2 expression in RILI. (A) Immunohistostaining for FPR2 in IR-exposed mouse lung tissue. Magnification, 1 × and 40 × . (B) Quantification of relative FPR2-stained area. (C) FPR2 mRNA expression in irradiated lung tissue measured via qRT-PCR. (D) Western blot analysis of FPR2 expression. (E) MT staining and immunohistostaining of FPR2 in specimens from patients with RILF. Data are expressed as the mean ± standard deviation (n = 3–5, *$p < 0.05$, **$p < 0.01$, and ***$p < 0.001$).

fewer areas of consolidation (Fig. 3A and B). As shown in Fig. 3E, the lung volume of apoptotic Jurkat cell–instilled mice were greater than that of the mice in the IR only group. MT staining results indicated that compared with the control group, the IR groups exhibited a marked increase in collagen contents (Fig. 3C and D). The group instilled with only apoptotic Jurkat cells exhibited significantly low collagen deposition compared to the other IR groups (Fig. 3C and D [$p < 0.05$]). Functional lung parameters evaluated here are listed in Table S1. The values of tissue damping (G) and elastance of the respiratory system (Ers) in the control group (4.94 ± 0.24 cm H_2O/mL [$p < 0.01$] and 32.43 ± 2.68 cm H_2O/mL [$p < 0.01$], respectively) were significantly lower than those in the IR only group (6.65 ± 0.65 cm H_2O/mL [$p < 0.01$] and 41.26 ± 0.73 cm H_2O/mL [$p < 0.01$], respectively). The values of inspiratory capacity and compliance of the respiratory system in the IR group showed a decreasing tendency, with increasing tendencies observed for Newtonian resistance, G, Ers, and resistance of the respiratory system (Fig. 3F). These results reflect the respiratory distress induced by IR in the IR group. However, this IR-induced respiratory distress in apoptotic Jurkat cell–instilled mice appeared significantly reversed. Furthermore, as shown in Fig. 3B and E, lung volumes in the IR + WRW4 and IR + Jur + WRW4 groups were lower than that in the IR + Jur group. Moreover, WRW4 administration reversed lung parameters, as assessed by the FlexiVent system, and worsened lung function (Fig. 3F). These results suggest that FPR2 expression enhanced by efferocytosis is involved in suppressing RILF.

3.4. Efferocytosis induced the upregulation of FPR2 expression and promoted inhibition of RILF

To explain the role of apoptotic Jurkat cell instillation and efferocytosis-induced FPR2 expression enhancement during the development of RILF, we examined the changes in EMT and ROS-related molecules and inflammatory cytokines. The stained area of α-SMA in the IR + WRW4 group significantly increased compared to that in the IR + Jur group ($p < 0.05$), and α-SMA expression in the IR + Jur + WRW4 group was higher than that in the IR + Jur group. However, α-SMA expression in the group with apoptotic Jurkat cell instillation decreased compared to that in the IR, IR + Jur + WRW4, and IR + WRW4 groups (Fig. 4A and B). Western blotting results confirmed that IR decreased the expression of the epithelial marker N-cadherin and increased those of α-SMA, vimentin, and the EMT marker Twist (Fig. 4C). Conversely, enhanced FPR2 expression restored the altered expression of these EMT-related molecules induced by IR (Fig. 4C). These results suggest that instillation of apoptotic Jurkat cells and enhanced FPR2 expression inhibit IR-induced EMT, thereby inhibiting RILF.

We also assessed the levels of ROS markers in this study. IR increased the expression of 8-OHdG; however, its expression levels in the IR + Jur group were significantly decreased ($p < 0.05$; Fig. 4A and B). Western blotting revealed higher expression levels of ROCK1 and NOX4 in the IR + Jur + WRW4 group than that in the IR + Jur group (Fig. 3C), suggesting that apoptotic Jurkat instillation and enhanced FPR2 expression have antioxidant capacity and attenuate damage caused by ROS. NF-κB, IL-1β, and TGF-β1 showed reduced expression in the IR + Jur group, whereas WRW4 reversed the expression of these (Fig. 4C). Thus, efferocytosis and enhanced FPR2 expression reduce an anti-inflammatory response by RILF.

4. Discussion

The administration of apoptotic cells ameliorates LPS-induced acute lung injury or sepsis [16]. To our knowledge, this study is

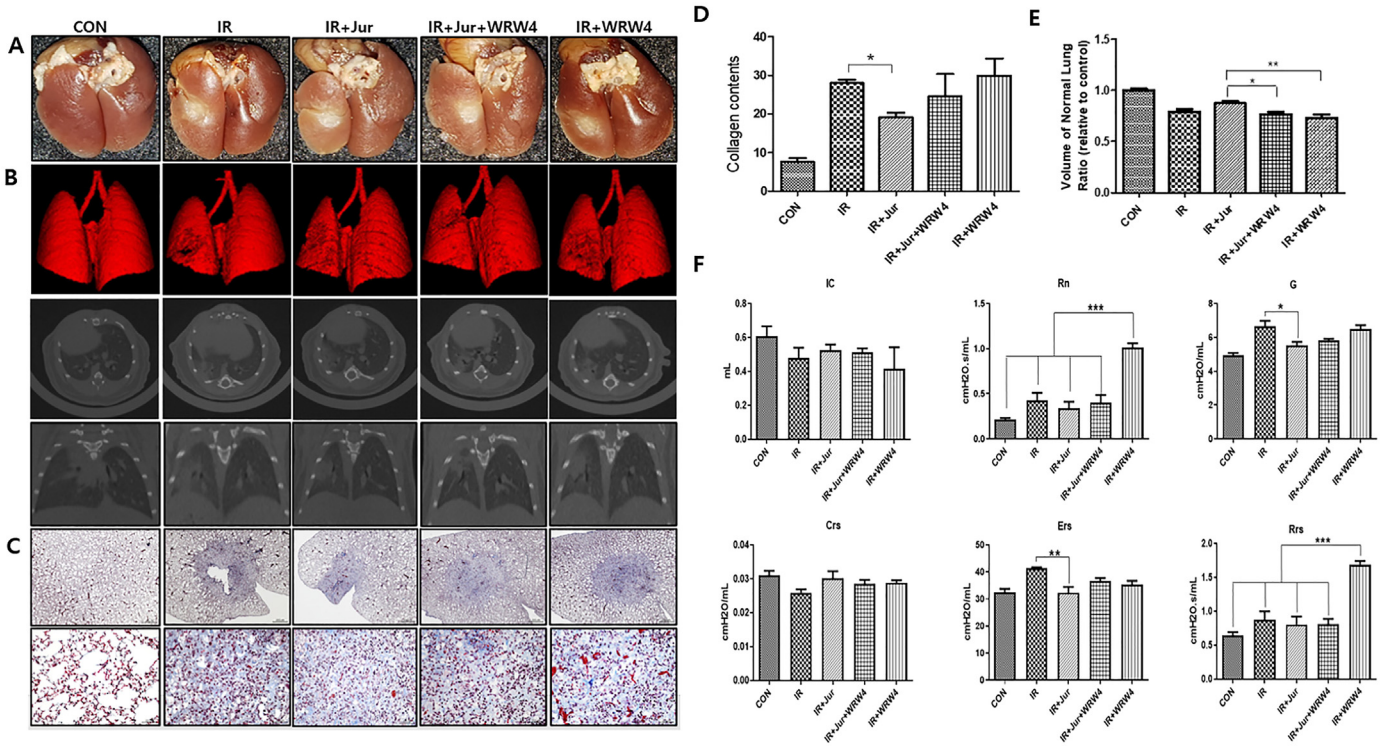

Fig. 3. Apoptotic Jurkat cell instillation attenuates RILF and rescues lung function. (A) Representative gross finding. (B) Micro-CT imaging. Representative micro-CT images of the lung of irradiated and control mice. 3D, horizontal, and *trans*-axial images. (C) Representative MT-stained image of mouse lung tissue. Magnification, 4 × and 40 × . (D) Quantification of MT-stained area. (E) Quantification of volume of normal left lung. (F) Functional measurements of mouse lungs were performed with the Flexivent system at six weeks after irradiation, was assessed. Data are expressed as the mean ± standard deviation (n = 3–5, $*p < 0.05$, $**p < 0.01$, $**p < 0.001$).

the first to demonstrate the effect of apoptotic cell instillation and enhanced FPR2 expression on RILI. We demonstrated that apoptotic Jurkat cell instillation exerts efferocytic effects to reduce pulmonary inflammation, fibrosis, EMT, and ROS while, interestingly, enhancing FPR2.

Intratracheal instillation of apoptotic Jurkat cells reduces lung fibrosis and inflammation in bleomycin-induced lung injury in mice [10,15], which suggests that apoptotic Jurkat cell signalling may protect against lung injuries related to dysregulated recovery processes [17]. The anti-fibrotic effects of apoptotic cells in this model depend on the induction of PPARγ expression in airway macrophages and increased production of HGF, which plays a key role in alveolar epithelial repair upon lung injury [10,15]. Interestingly, herein, FPR2 expression was predicted to exert these effects. Following administration of apoptotic Jurkat cells, the expression of FPR2 protein and mRNA significantly increased ($p < 0.05$, Fig. 2.).

Apoptotic cells can suppress macrophage inflammatory responses *in vitro*, indicating that efferocytosis plays a crucial role in modulating the inflammatory response of macrophages to promote resolution [18]. There are two subtypes of macrophages with distinct functions, M1-activated and M2-alternatively activated macrophages. M2 macrophages are activated by Th2 cytokines and are related to IR-induced fibrotic processes [19]. Our results indicated that apoptotic cell instillation and enhanced FPR2 expression significantly reduced the expression of macrophages and inflammatory cell infiltration and increased phagocytosis marker expression, consistent with previous findings [20]. However, further experiments regarding M1/M2 macrophage polarisation by instillation of apoptotic Jurkat cell and enhanced FPR2 expression are necessary to confirm these effects.

FPR2 attenuates hypoxia-induced lung injury [21]. HGF suppresses inflammation and protects epithelial cells from apoptosis [22]. FPR2 administration in a bleomycin-induced liver cirrhosis mouse model increased HGF expression [23], and apoptotic cell instillation inhibited EMT in lung alveolar epithelial cells via HGF expression [24]. Our results demonstrated that efferocytosis by apoptotic Jurkat instillation and enhanced FPR2 expression decreased the expression levels of inflammation cytokines, such as IL-6, NF-κB, IL-1β, and TGF-β1, decreased inflammatory cell infiltration, and increased HGF levels (Fig. 4C).

Clinical pulmonary fibrosis is diagnosed by micro-CT and lung function tests. Characteristic CT features of RILF include ground-glass opacity and consolidation, which were observed at 6 weeks post-IR in irradiated mice in the present study. Apoptotic Jurkat instillation resulted in partial resolution of these features (Fig. 3). FlexiVent® directly evaluates lung function using the same functional parameters as those used in humans [25]. Herein, apoptotic Jurkat cell–injected mice exhibited significantly better values of lung function parameters, including G and Ers comparing to IR mice. Interestingly, co-administration of apoptotic Jurkat cells and WRW4 reduced the effects of anti-pulmonary fibrosis. The results of micro-CT and FlexiVent® analyses correlated with our histopathological findings, indicating a critical role for efferocytosis and enhanced FPR2 expression in lung fibrosis.

EMT is an underlying mechanism of tissue fibrosis, wherein myofibroblasts are generated that serve as the primary source of extracellular matrix production from tissue epithelial cells [26]. Myofibroblasts are key mediators of lung fibrosis and can be generated from epithelial cells [27]. The expression levels N-cadherin, α-SMA, vimentin, and Twist were decreased in the apoptotic Jurkat cell–instilled group (Fig. 4), indicating that efferocytosis by apoptotic Jurkat instillation and enhanced FPR2 expression have anti-EMT effects. FPR2 expression attenuates mechanical stretch–induced pulmonary fibrosis via EMT.

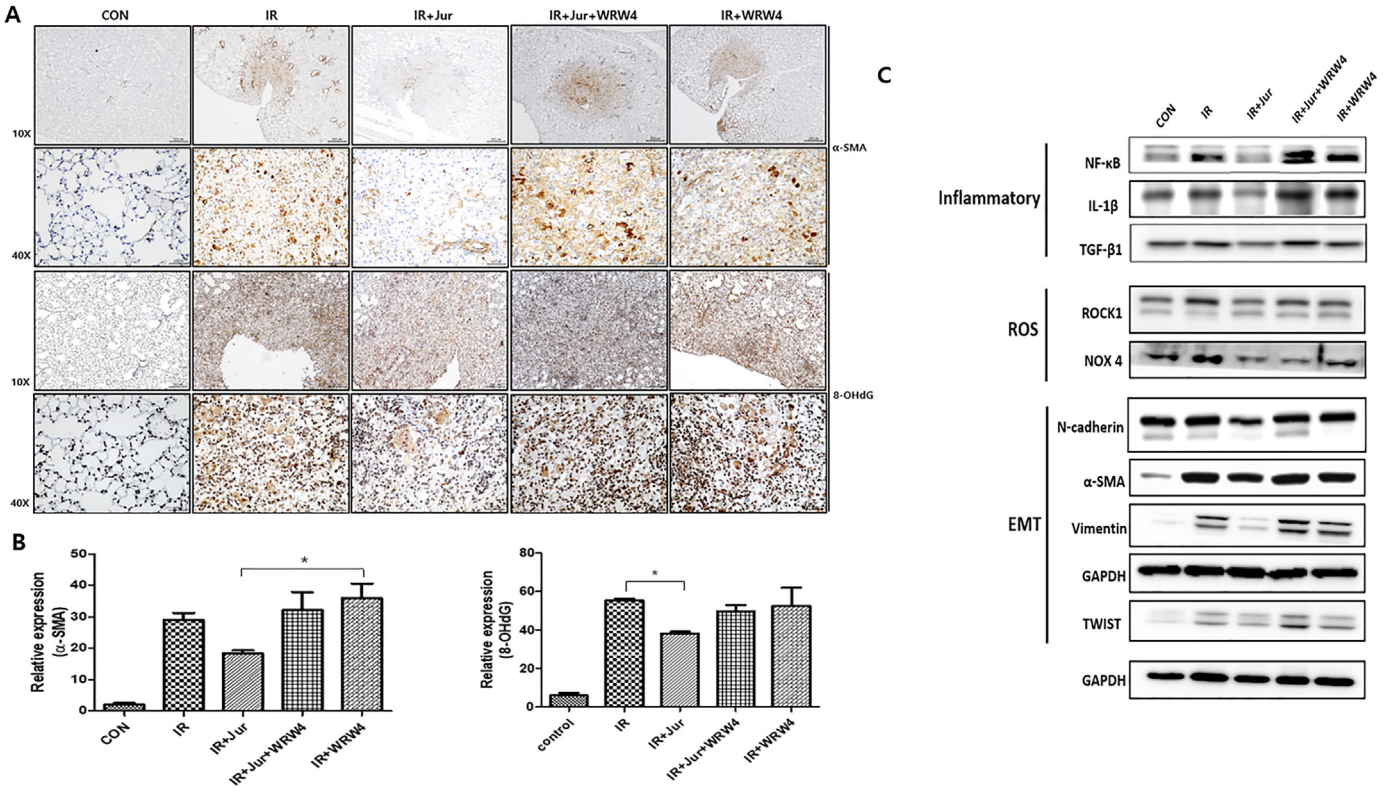

Fig. 4. Inhibitory effect of efferocytosis and enhanced FPR2 expression on EMT, ROS, and inflammation-related molecules in IR-lung tissue. (A) Representative immunohistochemical image and quantification of IR-lung tissues stained with antibodies against used α-SMA 8-OHdG. Magnification, 10 × and 40 × . (B) Quantification of α-SMA– and 8-OHdG–stained area. (C) Western blotting analysis of NF-κB, IL-1β, TGF-β1, ROCK1, NOX4, N-cadherin, α-SMA, vimentin, Twist, and GAPDH expression. Data are expressed as the mean ± standard deviation (n = 3–5, $*p < 0.05$).

ROS promotes to enhance the fibrotic response in the lungs. Members of the NOX family can serve as important sources of intracellular ROS, and NOX4 plays a key role in the development of lung fibrosis [28]. 8-OHdG and NOX4 expression is increased by IR [4], and inhibition of NOX4 expression decreases IR-induced differentiation of fibroblasts [29]. Our results showed that efferocytosis and enhanced FPR2 expression attenuate the level of 8-OHdG and expression of ROCK1 and NOX4 (Fig. 4), thereby, suggesting that efferocytosis by apoptotic Jurkat instillation and enhanced FPR2 expression may have antioxidant properties.

The relationship between enhanced FPR2 expression and efferocytosis is unclear, but there could be some relationship between the two in suppressing lung inflammation, fibrosis, EMT, ROS, and lung function in the RILI model. The mechanisms by which efferocytosis and enhanced FPR2 expression reduce RILI after apoptotic Jurkat cell instillation remain unclear; thus, further study is needed to elucidate the specific mechanisms involved in radiation-induced and FPR2-mediated fibrosis for the development of therapeutic agents. FPR2 expression was enhanced following apoptotic cell instillation, which led to reduced RILI, and the available experimental data suggest the feasibility of targeting FPR2 to RILI and RILF. Our study is providing evidence for promising clinical potential applications.

Declaration of competing interest

The authors declare that they have no conflict of interest.

Acknowledgments

This work was supported by grant from the National Research Foundation of Korea (NRF) [grant numbers NRF-2019R1A2C2086448, NRF-2020M2D9A2093976 and 2021R1I1A1A01044625].

Appendix A. Supplementary data

Supplementary data to this article can be found online at https://doi.org/10.1016/j.bbrc.2022.02.075.

References

[1] H. Jin, Y. Yoo, Y. Kim, Y. Kim, J. Cho, Y.S. Lee, Radiation-induced lung fibrosis: preclinical animal models and therapeutic strategies, Cancers (Basel) 12 (2020), https://doi.org/10.3390/cancers12061561.
[2] N. Dufton, R. Hannon, V. Brancaleone, J. Dalli, H.B. Patel, M. Gray, F. D'Acquisto, J.C. Buckingham, M. Perretti, R.J. Flower, Anti-inflammatory role of the murine formyl-peptide receptor 2: ligand-specific effects on leukocyte responses and experimental inflammation, J. Immunol. 184 (2010) 2611–2619, https://doi.org/10.4049/jimmunol.0903526.
[3] H.J. Lee, M.K. Park, E.J. Lee, C.H. Lee, Resolvin D1 inhibits TGF-beta1-induced epithelial mesenchymal transition of A549 lung cancer cells via lipoxin A4 receptor/formyl peptide receptor 2 and GPR32, Int. J. Biochem. Cell Biol. 45 (2013) 2801–2807, https://doi.org/10.1016/j.biocel.2013.09.018.
[4] H. Kim, S.H. Park, S.Y. Han, Y.S. Lee, J. Cho, J.M. Kim, LXA(4)-FPR2 signaling regulates radiation-induced pulmonary fibrosis via crosstalk with TGF-beta/Smad signaling, Cell Death Dis. 11 (2020), https://doi.org/10.1038/s41419-020-02846-7. ARTN 653.
[5] D.R. Korns, S.C. Frasch, R. Fernandez-Boyanapalli, P.M. Henson, et al., Modulation of macrophage efferocytosis in inflammation, Front. Immunol. 2 (2011) 57, https://doi.org/10.3389/fimmu.2011.00057.
[6] L Sun, H Zhou, Q Yan, L Wang, Q Liang, R.D. Ye, Ex vivo and in vitro effect of serum amyloid a in the induction of macrophage M2 markers and efferocytosis of apoptotic neutrophils, J. Immunol. 194 (2015) 4891–4900, https://doi.org/10.4049/jimmunol.1402164.
[7] A. Ortega-Gomez, M. Perretti, O. Soehnlein, Resolution of inflammation: an integrated view, EMBO Mol. Med. 5 (2013) 661–674, https://doi.org/10.1002/emmm.201202382.
[8] F. Abedi, A.W. Hayes, R. Reiter, G.J.P.r. Karimi, Acute Lung Injury: the

Therapeutic Role of Rho Kinase Inhibitors, vol. 155, 2020, p. 104736.
[9] J. Milara, G. Hernandez, B. Ballester, A. Morell, I. Roger, P. Montero, J. Escriva, J.M. Lloris, M. Molina-Molina, E. Morcillo, J. Cortijo, The JAK2 pathway is activated in idiopathic pulmonary fibrosis, Respir. Res. 19 (2018) 24, https://doi.org/10.1186/s12931-018-0728-9.
[10] Y.S. Yoon, S.Y. Kim, M.J. Kim, J.H. Lim, M.S. Cho, J.L. Kang, PPARgamma activation following apoptotic cell instillation promotes resolution of lung inflammation and fibrosis via regulation of efferocytosis and proresolving cytokines, Mucosal Immunol. 8 (2015) 1031–1046, https://doi.org/10.1038/mi.2014.130.
[11] H.A. Chapman, Epithelial-mesenchymal Interactions in Pulmonary Fibrosis, vol. 73, 2011, pp. 413–435.
[12] S. Piera-Velazquez, F.A. Mendoza, S.A. Jimenez, Endothelial to mesenchymal transition (EndoMT) in the pathogenesis of human fibrotic diseases, J. Clin. Med. 5 (2016), https://doi.org/10.3390/jcm5040045.
[13] J.Y. Kim, D. Shin, G. Lee, J.M. Kim, D. Kim, Y.M. An, B.R. Yoo, H. Chang, M. Kim, J. Cho, H. Bae, Standardized herbal formula PM014 inhibits radiation-induced pulmonary inflammation in mice, Sci. Rep. 7 (2017) 45001, https://doi.org/10.1038/srep45001.
[14] H. Jin, S. Jeon, G.Y. Kang, H.J. Lee, J. Cho, Y.S. Lee, Identification of radiation response genes and proteins from mouse pulmonary tissues after high-dose per fraction irradiation of limited lung volumes, Int. J. Radiat. Biol. 93 (2017) 184–193, https://doi.org/10.1080/09553002.2017.1235297.
[15] Y.-J. Lee, C. Moon, S.H. Lee, H.-J. Park, J.-Y. Seoh, M.-S. Cho, J.L. Kang, Apoptotic cell instillation after bleomycin attenuates lung injury through hepatocyte growth factor induction, Eur. Respir. J. 40 (2012) 424–435.
[16] Y. Ren, Y. Xie, G. Jiang, J. Fan, J. Yeung, W. Li, P.K. Tam, J. Savill, Apoptotic cells protect mice against lipopolysaccharide-induced shock, J. Immunol. 180 (2008) 4978–4985.
[17] A.M. Grabiec, T. Hussell, The role of airway macrophages in apoptotic cell clearance following acute and chronic lung inflammation, Semin. Immunopathol. 38 (2016) 409–423, https://doi.org/10.1007/s00281-016-0555-3.
[18] P. Saas, S. Kaminski, S. Perruche, Prospects of apoptotic cell-based therapies for transplantation and inflammatory diseases, Immunotherapy 5 (2013) 1055–1073, https://doi.org/10.2217/imt.13.103.
[19] H. Zhang, G. Han, H. Liu, J. Chen, X. Ji, F. Zhou, Y. Zhou, C. Xie, The development of classically and alternatively activated macrophages has different effects on the varied stages of radiation-induced pulmonary injury in mice, J. Radiat. Res. 52 (2011) 717–726, https://doi.org/10.1269/jrr.11054.
[20] J.W. Kang, S.M. Lee, Resolvin D1 protects the liver from ischemia/reperfusion injury by enhancing M2 macrophage polarization and efferocytosis, Biochim. Biophys. Acta 1861 (2016) 1025–1035, https://doi.org/10.1016/j.bbalip.2016.06.002.
[21] Y.E. Kim, W.S. Park, S.Y. Ahn, D.K. Sung, S.I. Sung, J.H. Kim, Y.S. Chang, WKYMVm hexapeptide, a strong formyl peptide receptor 2 agonist, attenuates hyperoxia-induced lung injuries in newborn mice, Sci. Rep. 9 (2019) 1–11.
[22] A. Kakazu, G. Chandrasekher, H.E. Bazan, HGF protects corneal epithelial cells from apoptosis by the PI-3K/Akt-1/Bad-but not the ERK1/2-mediated signaling pathway, Invest. Ophthalmol. Vis. Sci. 45 (2004) 3485–3492.
[23] J.H. Jun, S.Y. Park, S. Park, H.J. Park, J.Y. Kim, G.T. Park, S.H. Bae, J.H. Kim, G.J. Kim, Formyl peptide receptor 2 alleviates hepatic fibrosis in liver cirrhosis by vascular remodeling, Int. J. Mol. Sci. 22 (2021) 2107.
[24] Y.-S. Yoon, Y.-J. Lee, Y.-H. Choi, Y.M. Park, J.L. Kang, Macrophages programmed by apoptotic cells inhibit epithelial-mesenchymal transition in lung alveolar epithelial cells via PGE 2, PGD 2, and HGF, Sci. Rep. 6 (2016) 1–18.
[25] J.A. Vanoirbeek, M. Rinaldi, V. De Vooght, S. Haenen, S. Bobic, G. Gayan-Ramirez, P.H. Hoet, E. Verbeken, M. Decramer, B. Nemery, Noninvasive and invasive pulmonary function in mouse models of obstructive and restrictive respiratory diseases, Am. J. Respir. Cell Mol. Biol. 42 (2010) 96–104.
[26] D.-h. Shin, H.-M. Park, K.-A. Jung, H.-G. Choi, J.-A. Kim, D.-D. Kim, S.G. Kim, K.W. Kang, S.K. Ku, T.W. Kensler, The NRF2–heme oxygenase-1 system modulates cyclosporin A-induced epithelial–mesenchymal transition and renal fibrosis, Free Radic. Biol. Med. 48 (2010) 1051–1063.
[27] H. Tanjore, X.C. Xu, V.V. Polosukhin, A.L. Degryse, B. Li, W. Han, T.P. Sherrill, D. Plieth, E.G. Neilson, T.S. Blackwell, Contribution of epithelial-derived fibroblasts to bleomycin-induced lung fibrosis, Am. J. Respir. Crit. Care Med. 180 (2009) 657–665.
[28] L. Hecker, R. Vittal, T. Jones, R. Jagirdar, T.R. Luckhardt, J.C. Horowitz, S. Pennathur, F.J. Martinez, V.J. Thannickal, NADPH oxidase-4 mediates myofibroblast activation and fibrogenic responses to lung injury, Nat. Med. 15 (2009) 1077–1081.
[29] Z.-Y. Hong, S.H. Eun, K. Park, W.H. Choi, J.I. Lee, E.-J. Lee, J.M. Lee, M.D. Story, J. Cho, Development of a small animal model to simulate clinical stereotactic body radiotherapy-induced central and peripheral lung injuries, J. Radiat. Res. 55 (2014) 648–657.